Supporting Information for "Evaluating climate models' cloud feedbacks against expert judgement"

Mark D. Zelinka[1], Stephen A. Klein[1], Yi Qin[1], Timothy A. Myers[1]

[1]Lawrence Livermore National Laboratory

Contents of this file

1. Figures S1 to S22

Introduction

In this document, we provide 22 supplementary figures. Figures S1 and S2 compare cloud radiative kernel-derived cloud feedbacks with those derived using independent methods. Figure S3 provides a matrix showing which regions and cloud types contribute to each feedback, facilitating understanding of how the assessed feedbacks are computed, which feedbacks are left unassessed, and how we further discretize these remaining unassessed feedbacks. Figures S4-S22 are identical to Figure 1 of the main text, but individual models are highlighted in each.

References

Huang, Y., Xia, Y., & Tan, X. X. (2017). On the pattern of CO2 radiative forcing and poleward energy transport. *Journal of Geophysical Research-Atmospheres*, *122*(20), 10578–10593. doi: 10.1002/2017jd027221

Shell, K. M., Kiehl, J. T., & Shields, C. A. (2008). Using the Radiative Kernel Technique to Calculate Climate Feedbacks in NCAR's Community Atmospheric Model. *J. Climate*, *21*(10), 2269–2282. doi: 10.1175/2007JCLI2044.1

Soden, B. J., Held, I. M., Colman, R., Shell, K. M., Kiehl, J. T., & Shields, C. A. (2008). Quantifying Climate Feedbacks Using Radiative Kernels. *J. Climate*, *21*, 3504–3520. doi: 10.1175/2007JCLI2110.1

Taylor, K. E., Crucifix, M., Braconnot, P., Hewitt, C. D., Doutriaux, C., Broccoli, A. J., ... Webb, M. J. (2007). Estimating Shortwave Radiative Forcing and Response in Climate Models. *J. Climate*, *20*(11), 2530–2543. doi: 10.1175/JCLI4143.1

Zelinka, M. D., Klein, S. A., & Hartmann, D. L. (2012). Computing and Partitioning Cloud Feedbacks Using Cloud Property Histograms. Part I: Cloud Radiative Kernels. *Journal of Climate*, *25*(11), 3715–3735. doi: 10.1175/jcli-d-11-00248.1

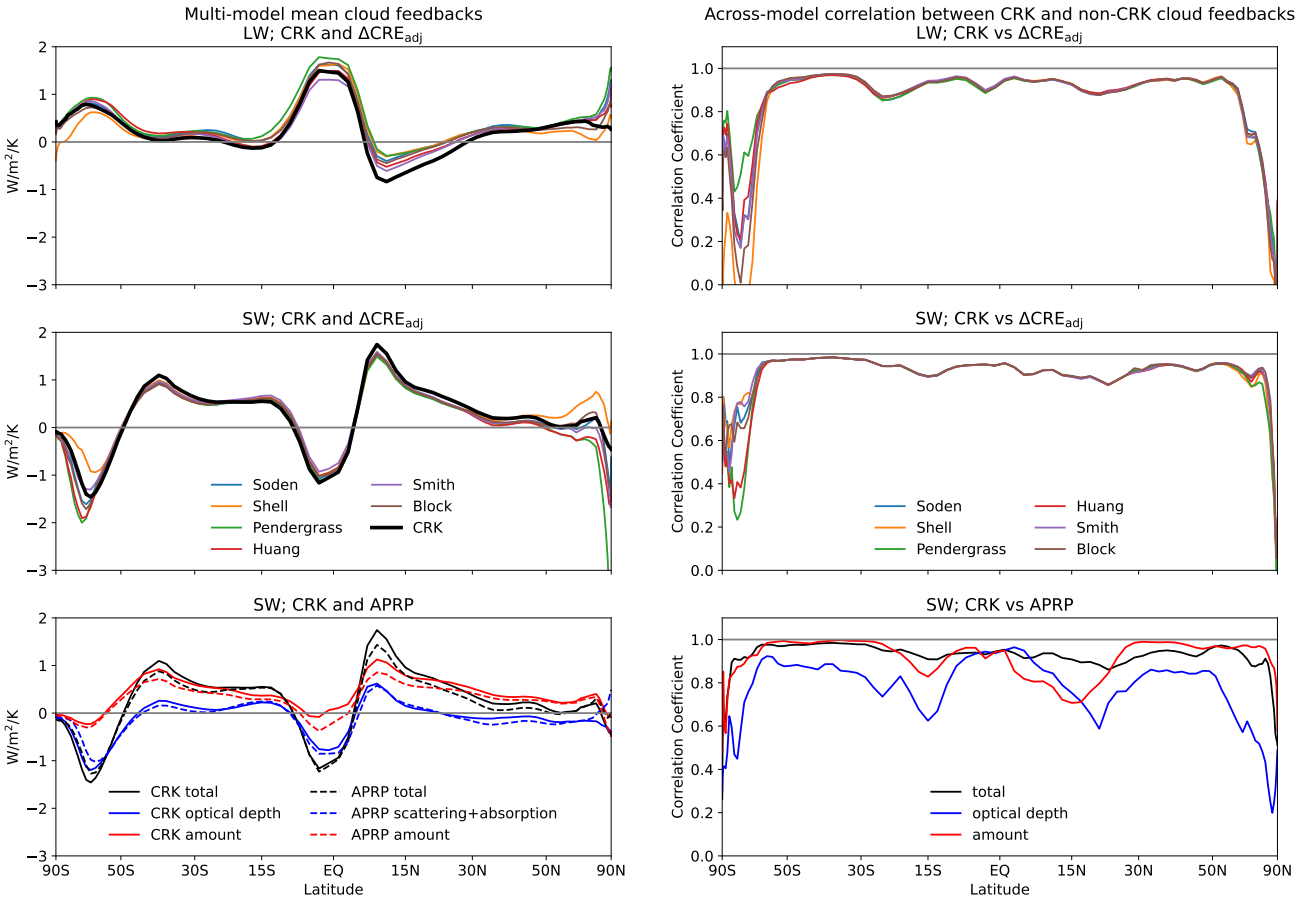

Figure S1. (left) Zonal and multi-model mean LW and SW cloud feedbacks estimated using three methodologies: cloud radiative kernels (CRK; Zelinka et al., 2012), adjusted change in cloud radiative effect (ΔCRE_{adj}; Soden et al., 2008; Shell et al., 2008), and approximate partial radiative perturbation (APRP; Taylor et al., 2007). Six estimates of ΔCRE_{adj} are shown, each using a different radiative kernel identified in the caption on row 2. (right) Across-model correlation between CRK-derived and non-CRK-derived zonal mean cloud feedbacks. The CRK-derived SW cloud feedback is further broken down into optical depth and amount components, which are compared to the APRP-derived SW scattering plus absorption component and amount component, respectively.

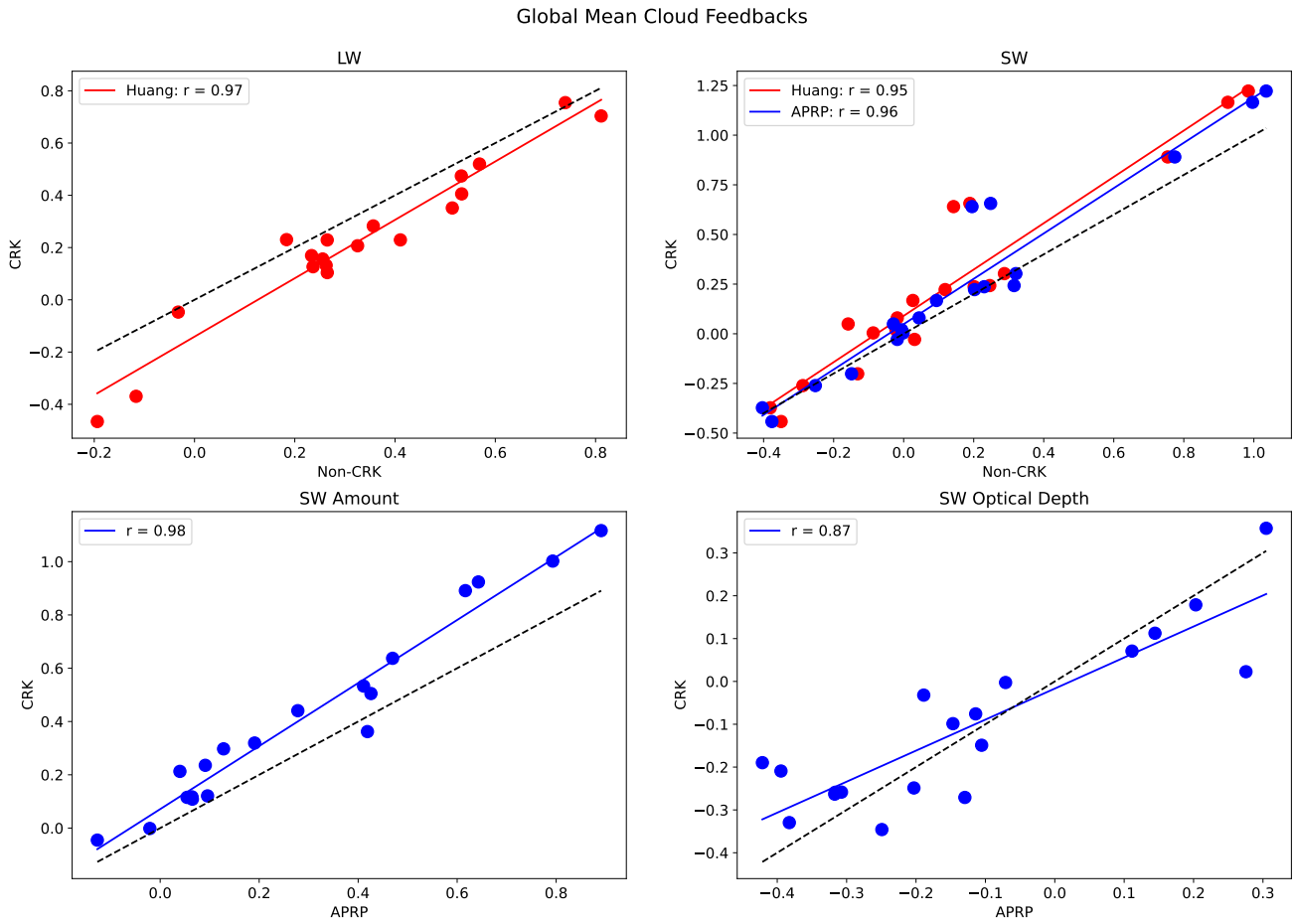

Figure S2. Global mean LW and SW cloud feedbacks estimated using the CRK method scattered against those estimated using non-CRK techniques. For clarity, we show only one of the six estimates of $\Delta\mathrm{CRE}_{\mathrm{adj}}$, that derived using the kernels of Huang et al. (2017).

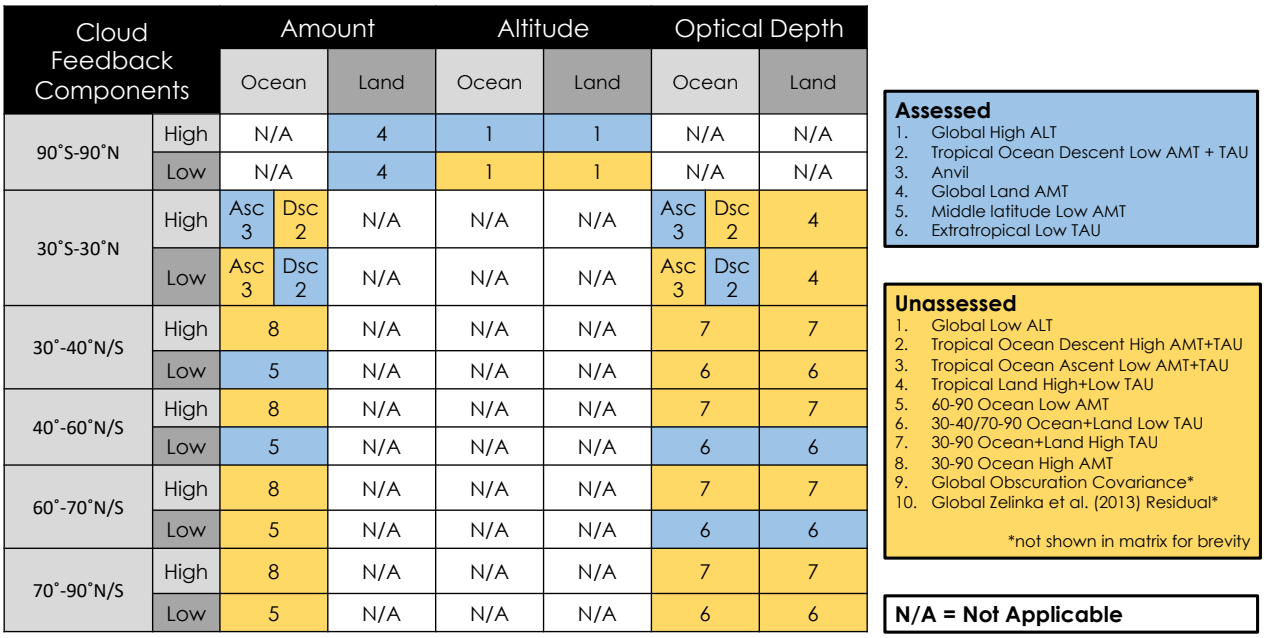

Figure S3. Matrix of assessed and unassessed cloud feedbacks. The sum of all assessed and unassessed components equals the total cloud feedback.

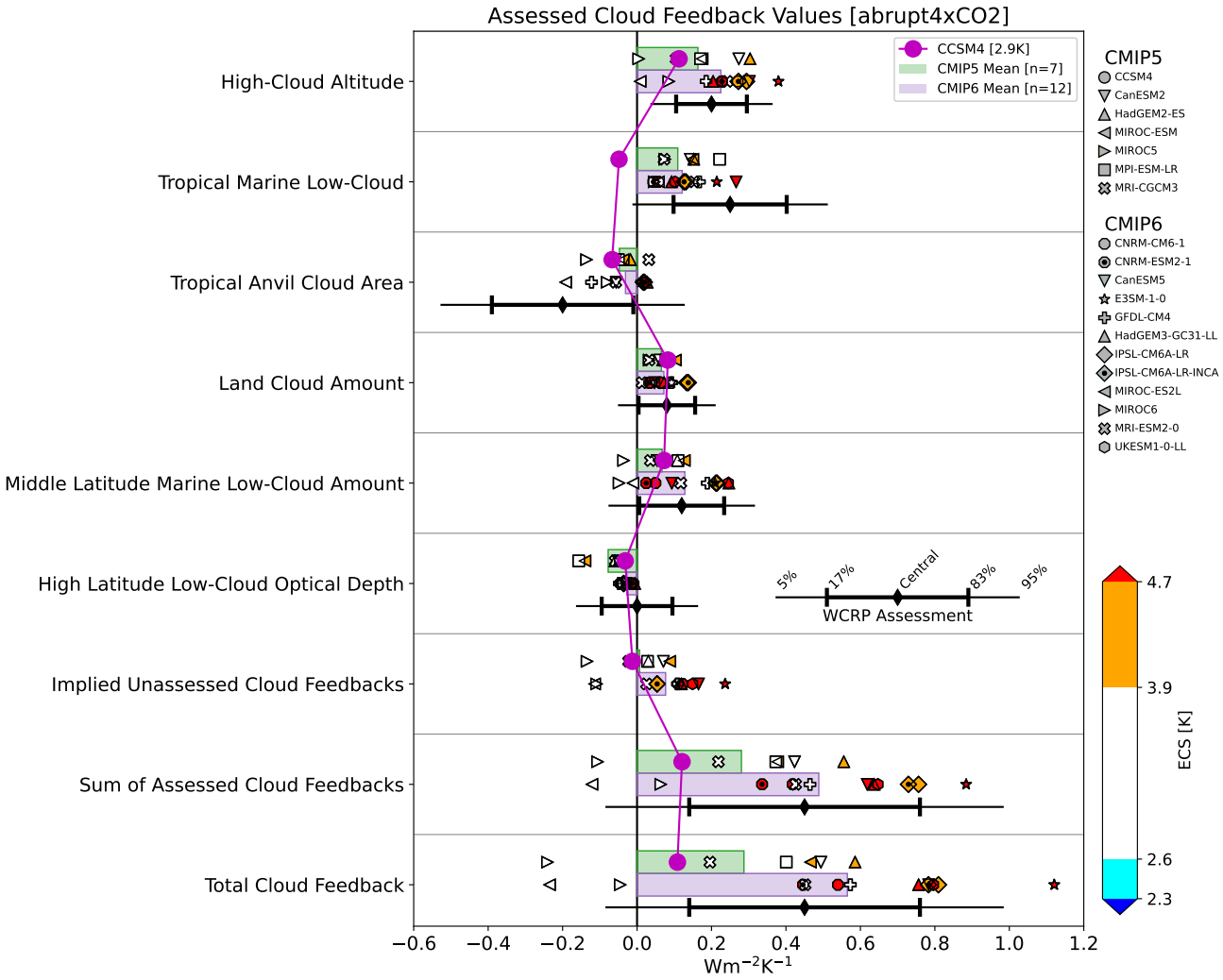

Figure S4. As in Figure 1, but highlighting CCSM4.

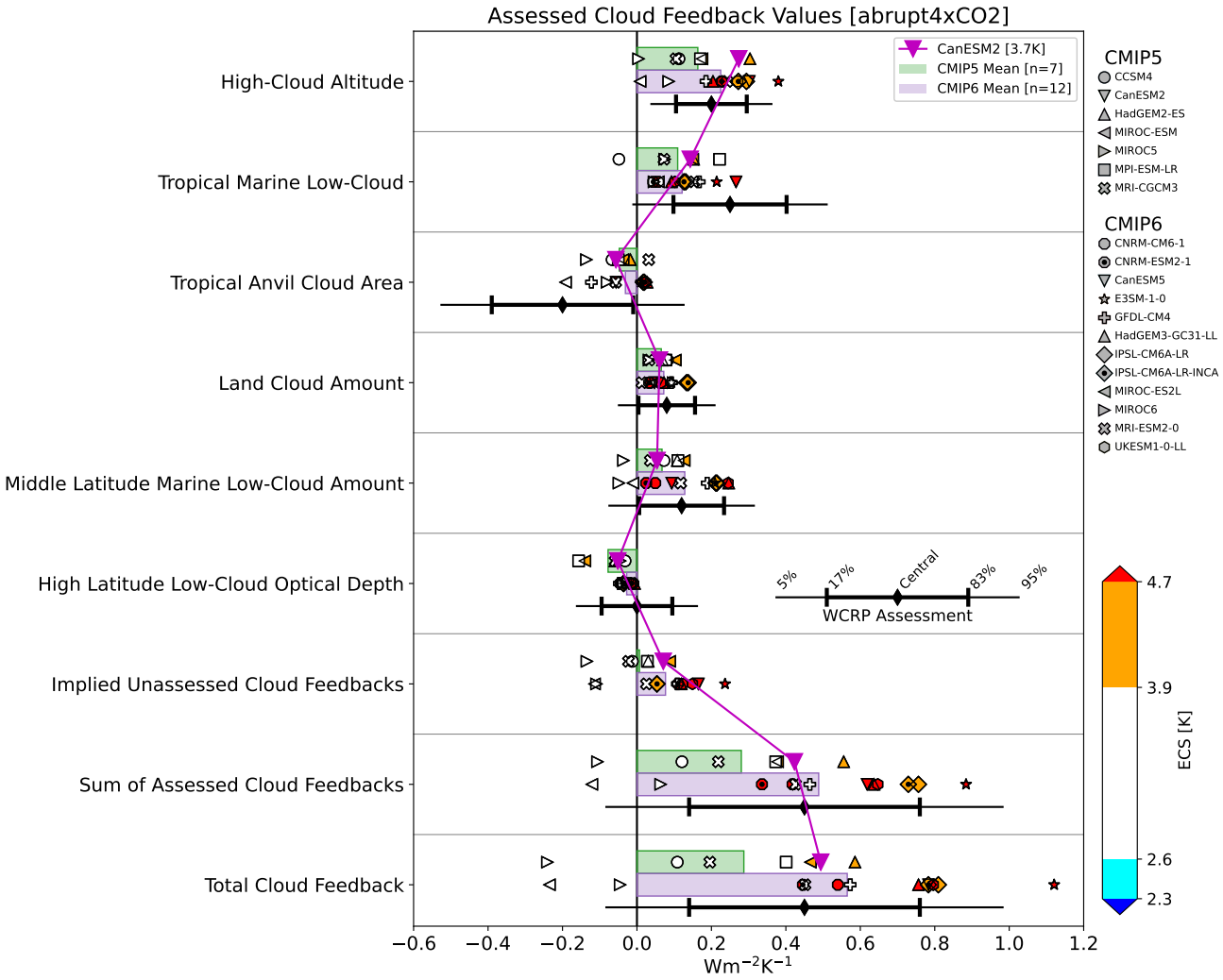

Figure S5. As in Figure 1, but highlighting CanESM2.

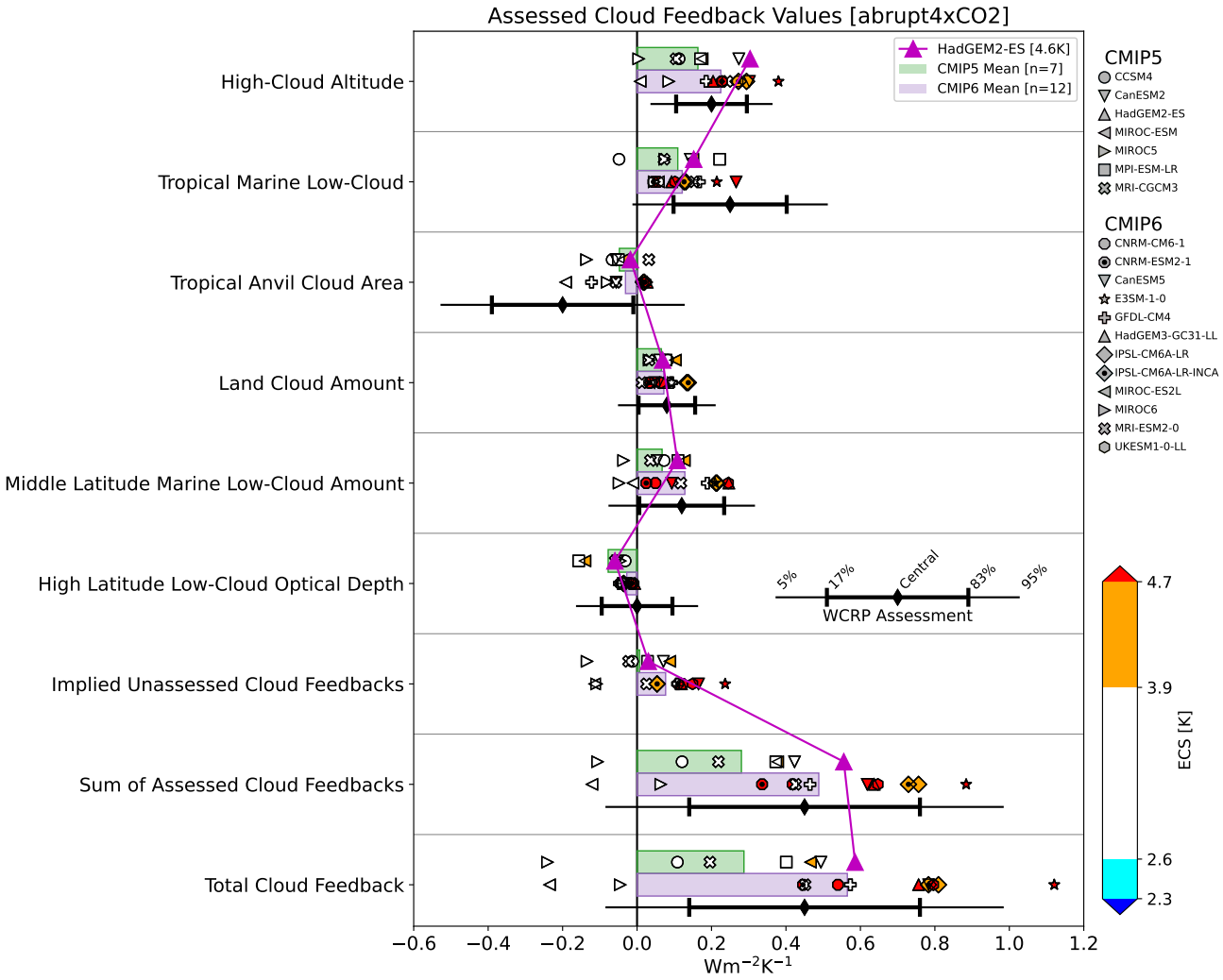

Figure S6. As in Figure 1, but highlighting HadGEM2-ES.

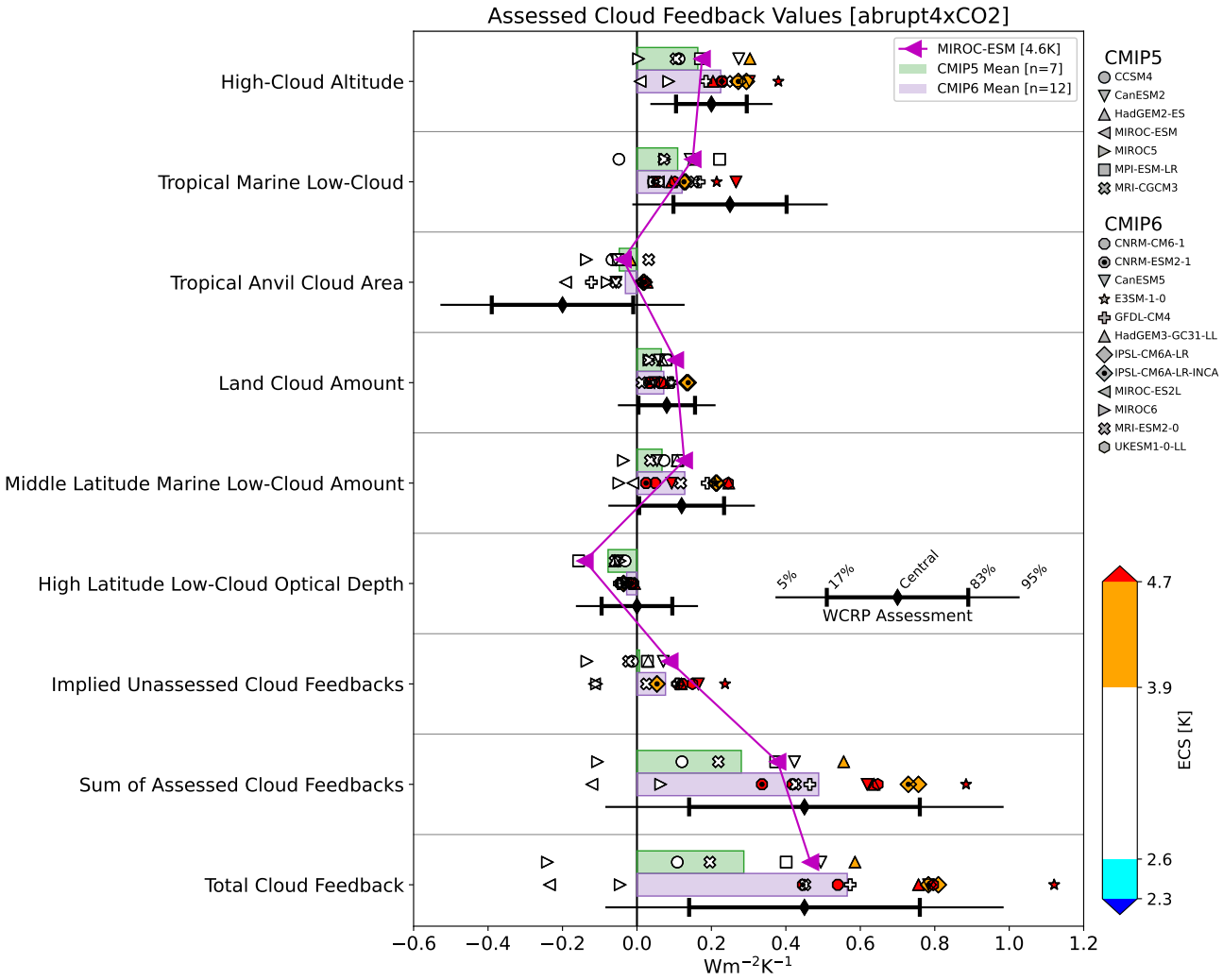

Figure S7. As in Figure 1, but highlighting MIROC-ESM.

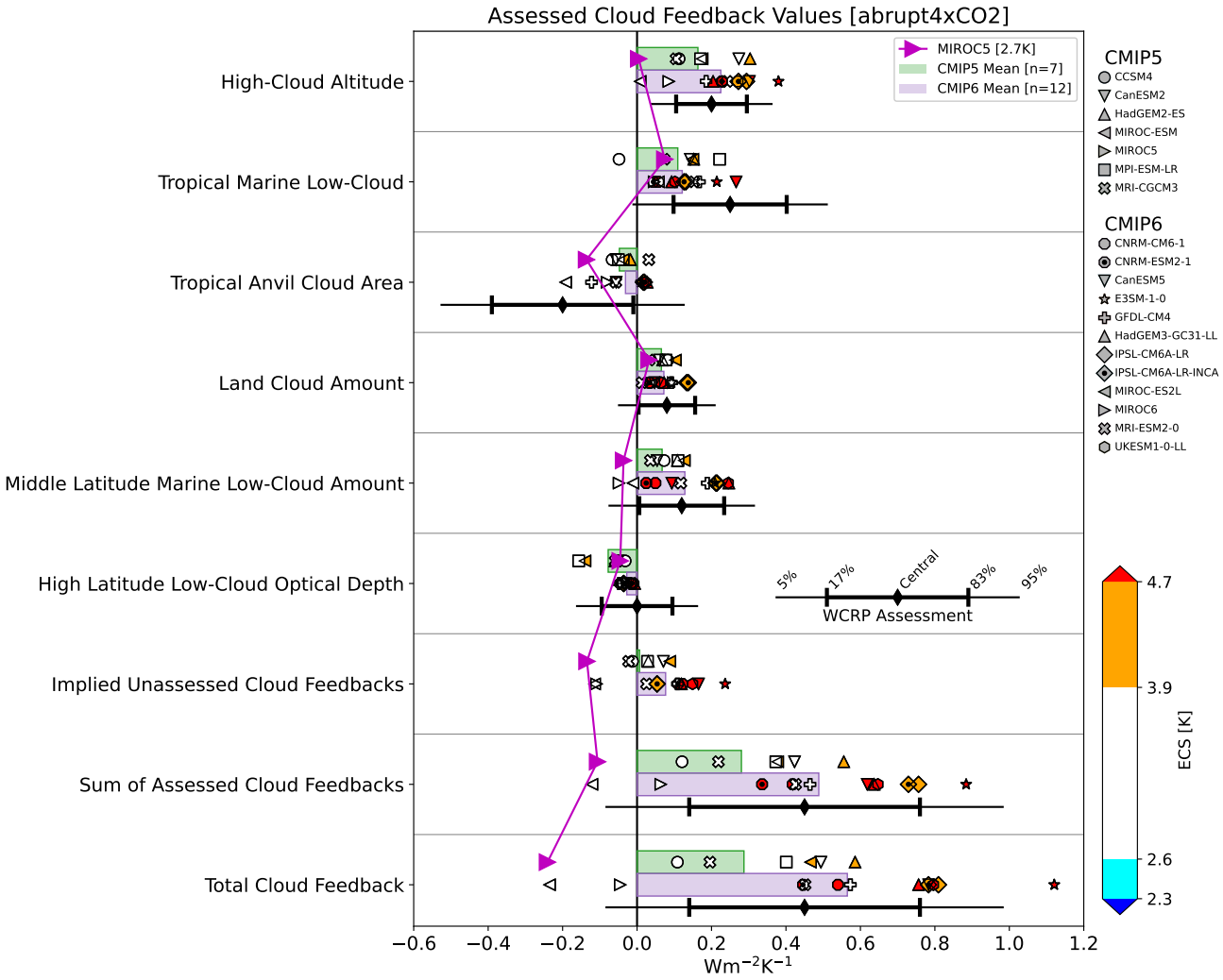

Figure S8. As in Figure 1, but highlighting MIROC5.

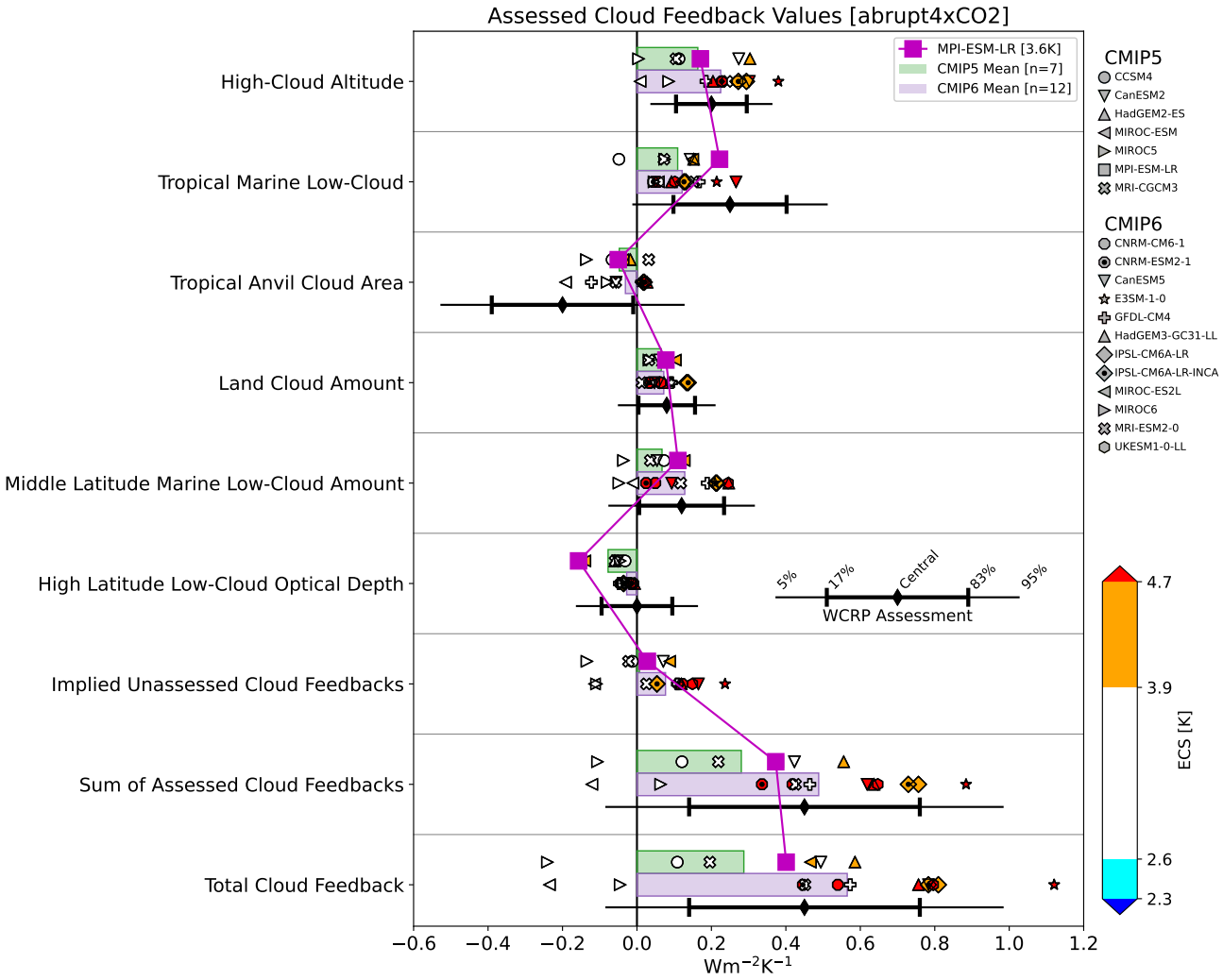

Figure S9. As in Figure 1, but highlighting MPI-ESM-LR.

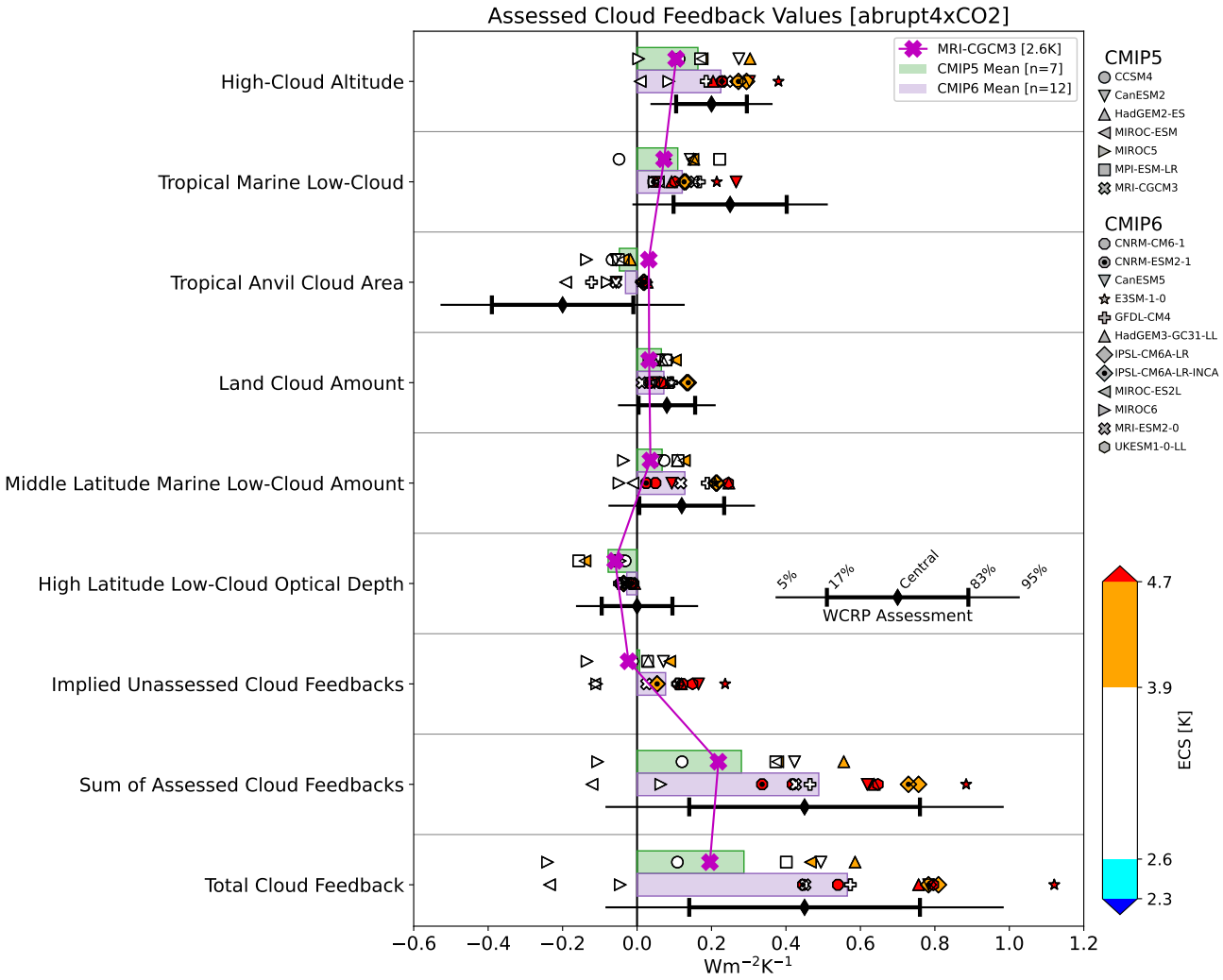

Figure S10. As in Figure 1, but highlighting MRI-CGCM3.

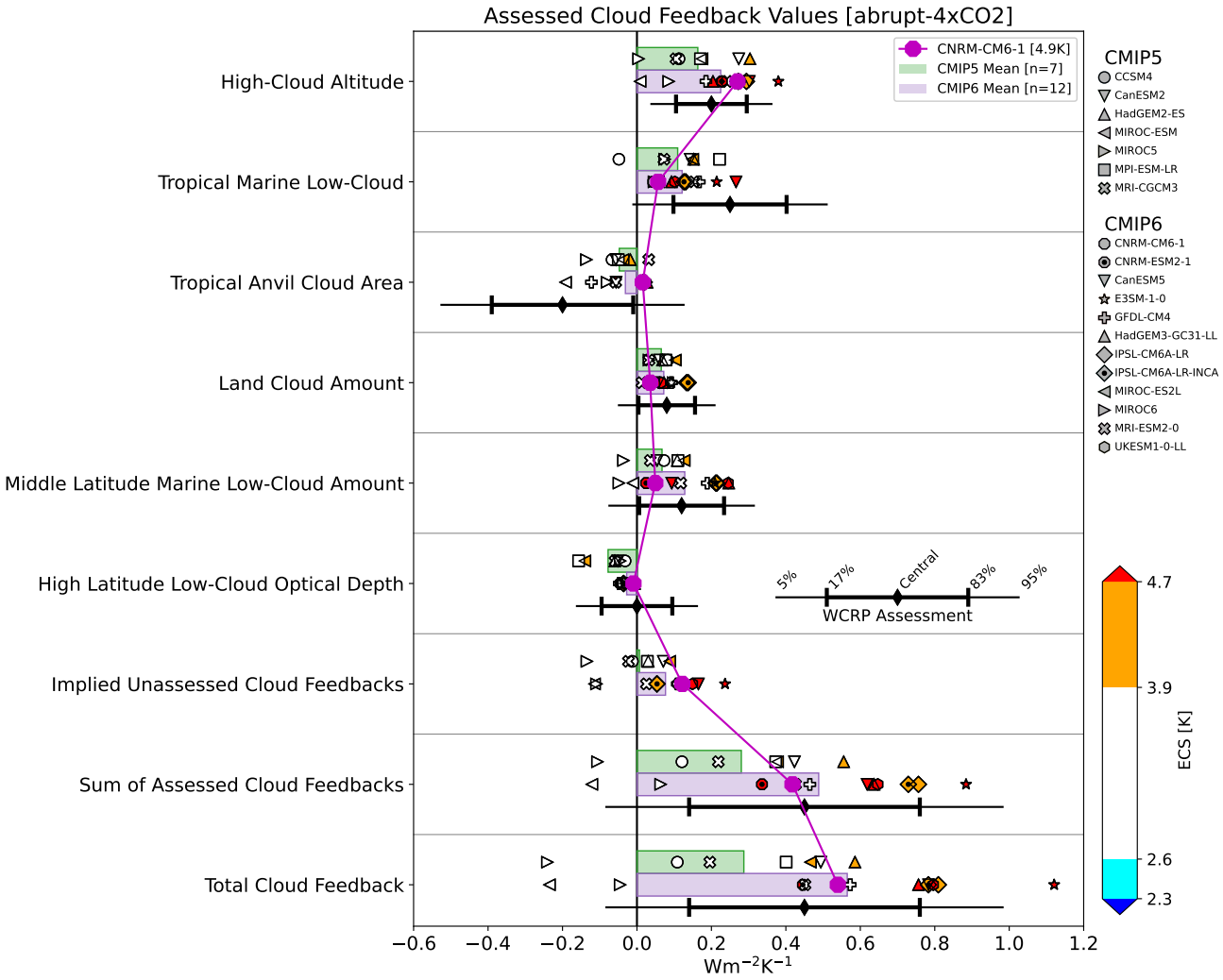

Figure S11. As in Figure 1, but highlighting CNRM-CM6-1.

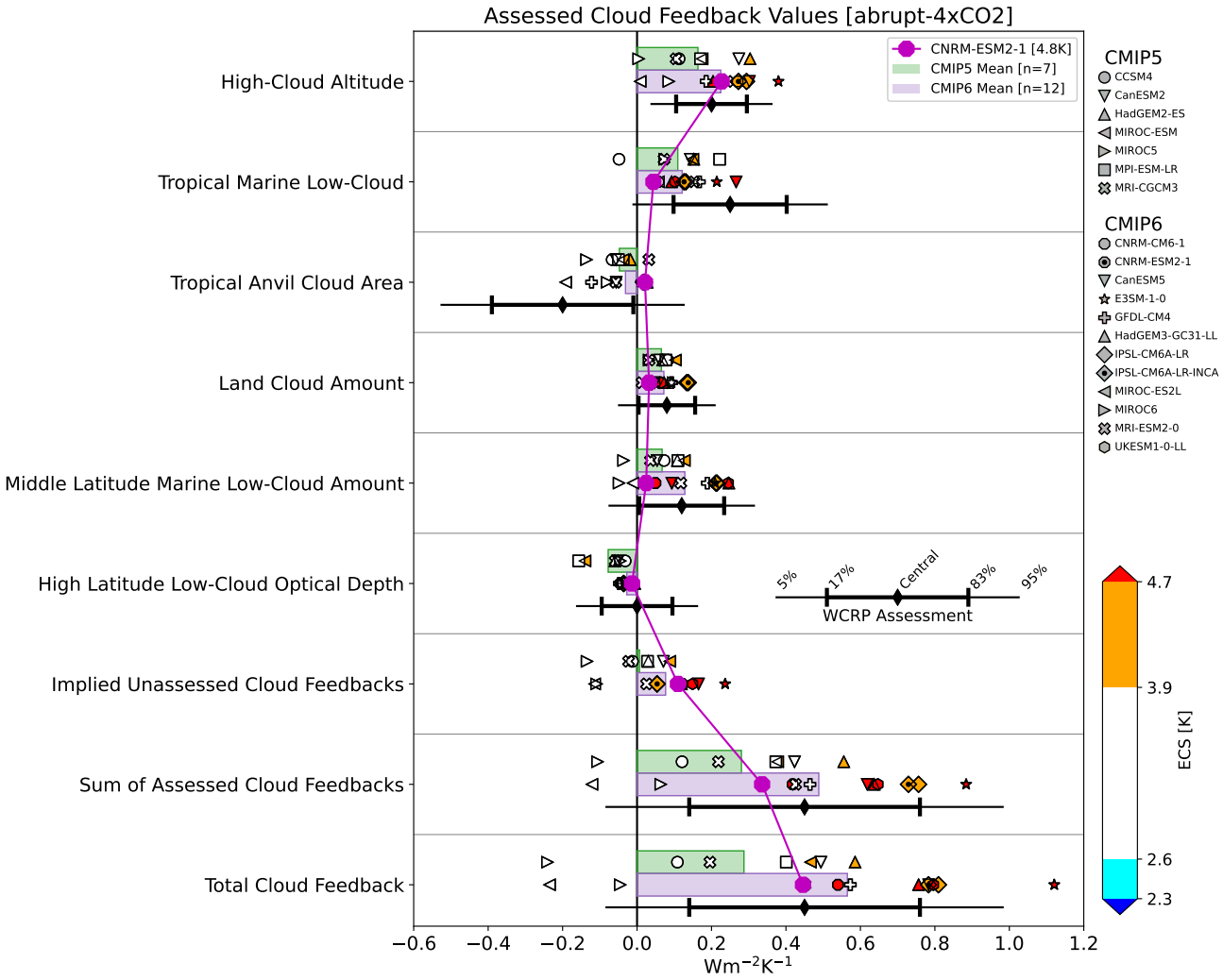

Figure S12. As in Figure 1, but highlighting CNRM-ESM2-1.

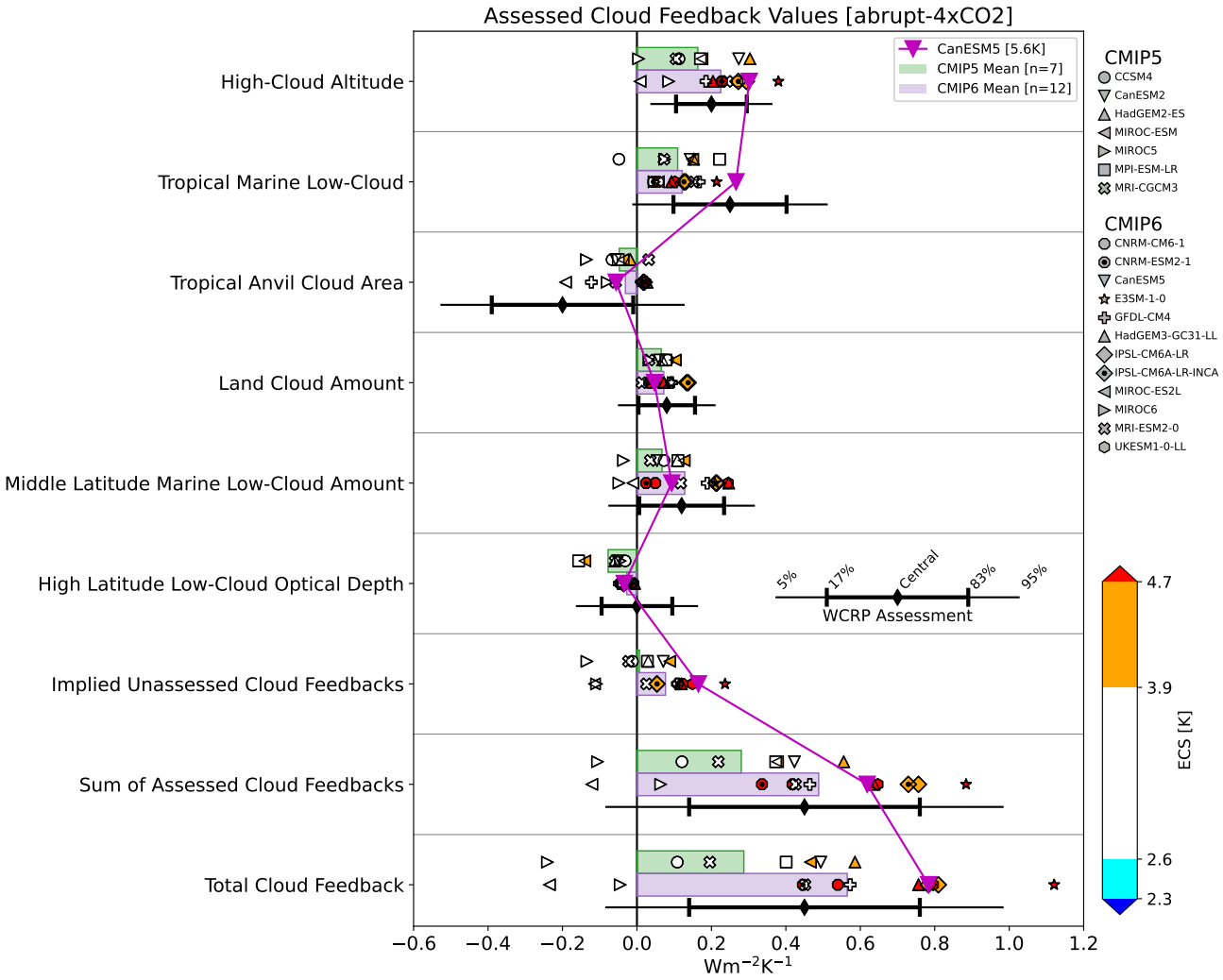

Figure S13. As in Figure 1, but highlighting CanESM5.

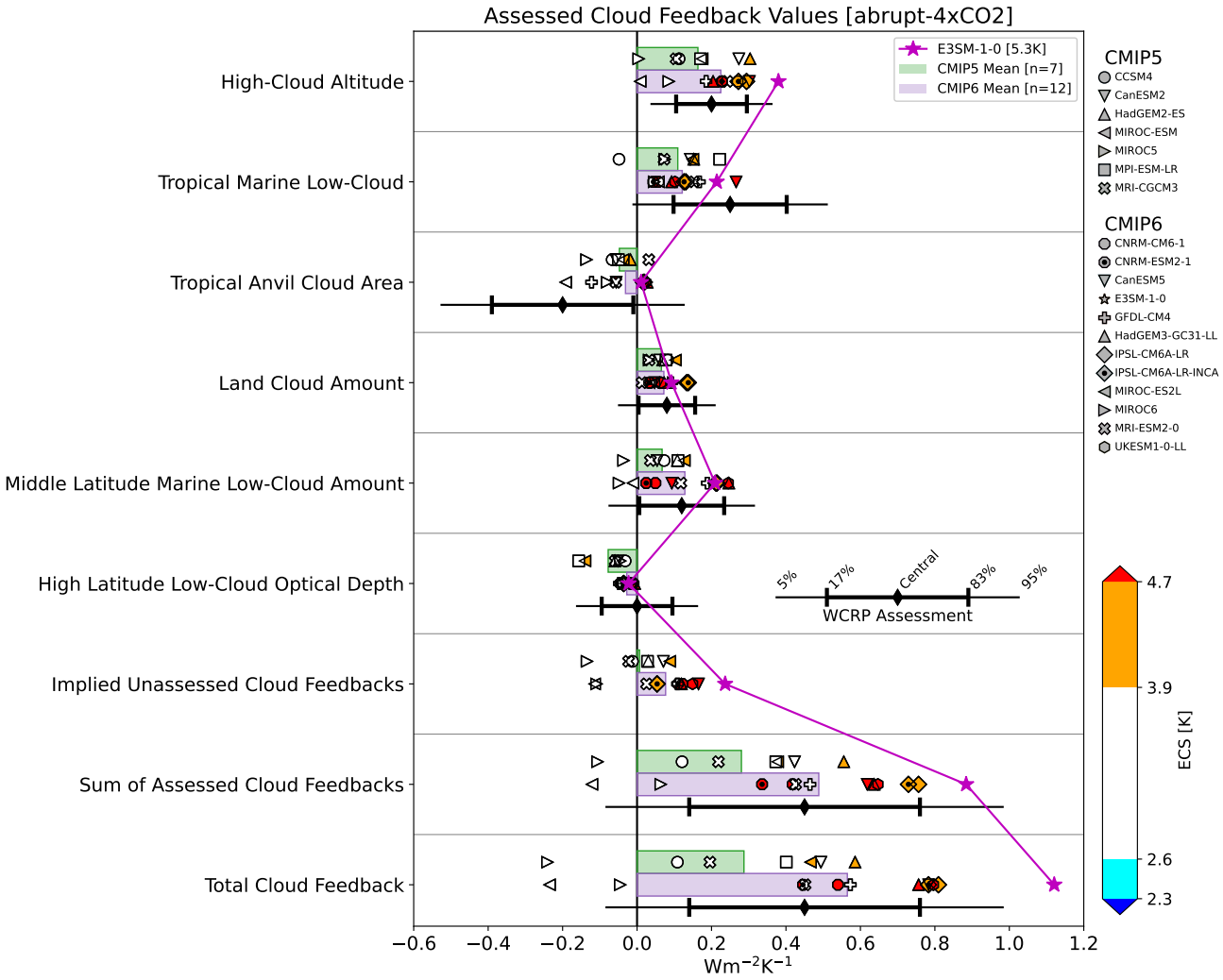

Figure S14. As in Figure 1, but highlighting E3SM-1-0.

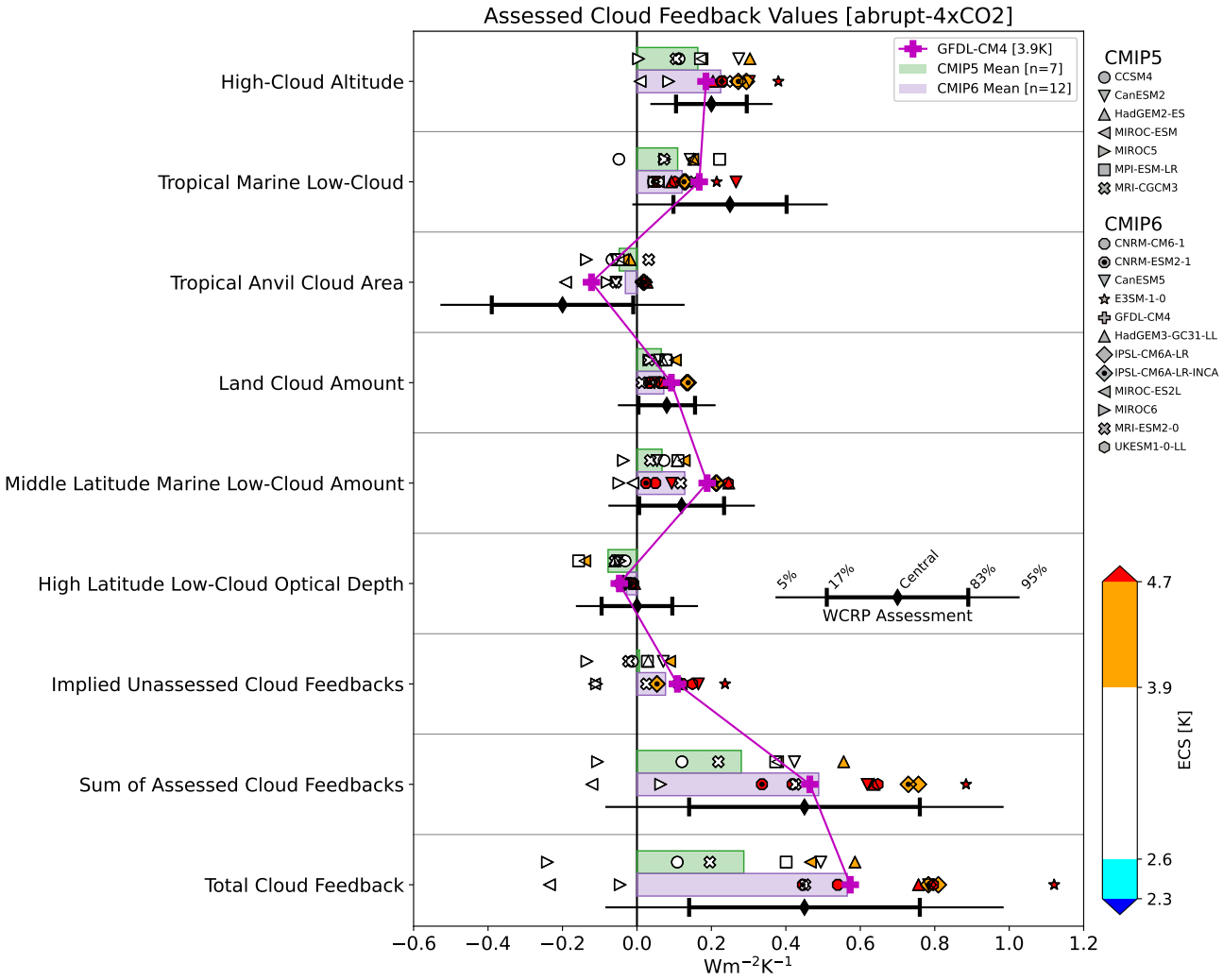

Figure S15. As in Figure 1, but highlighting GFDL-CM4.

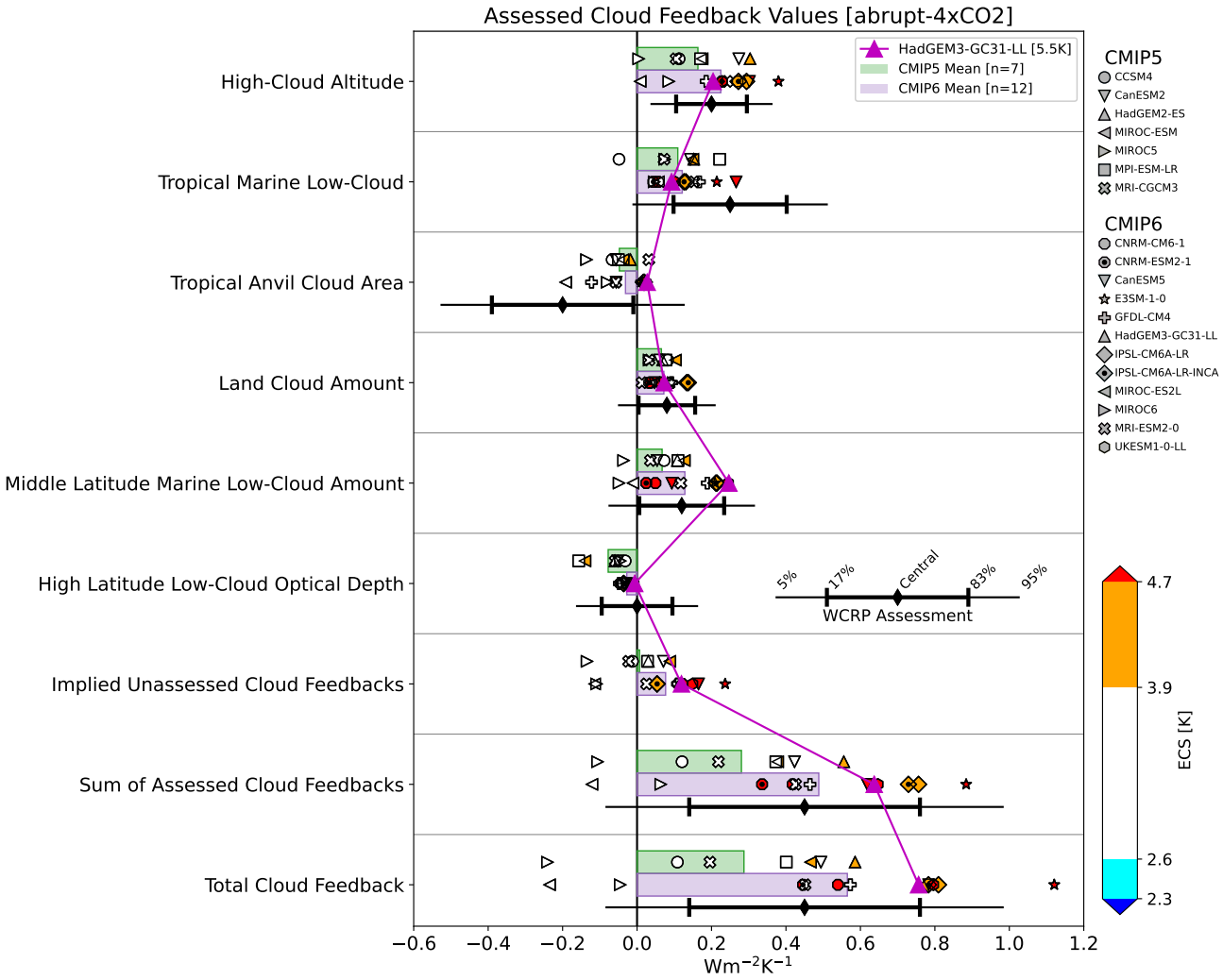

Figure S16. As in Figure 1, but highlighting HadGEM3-GC31-LL.

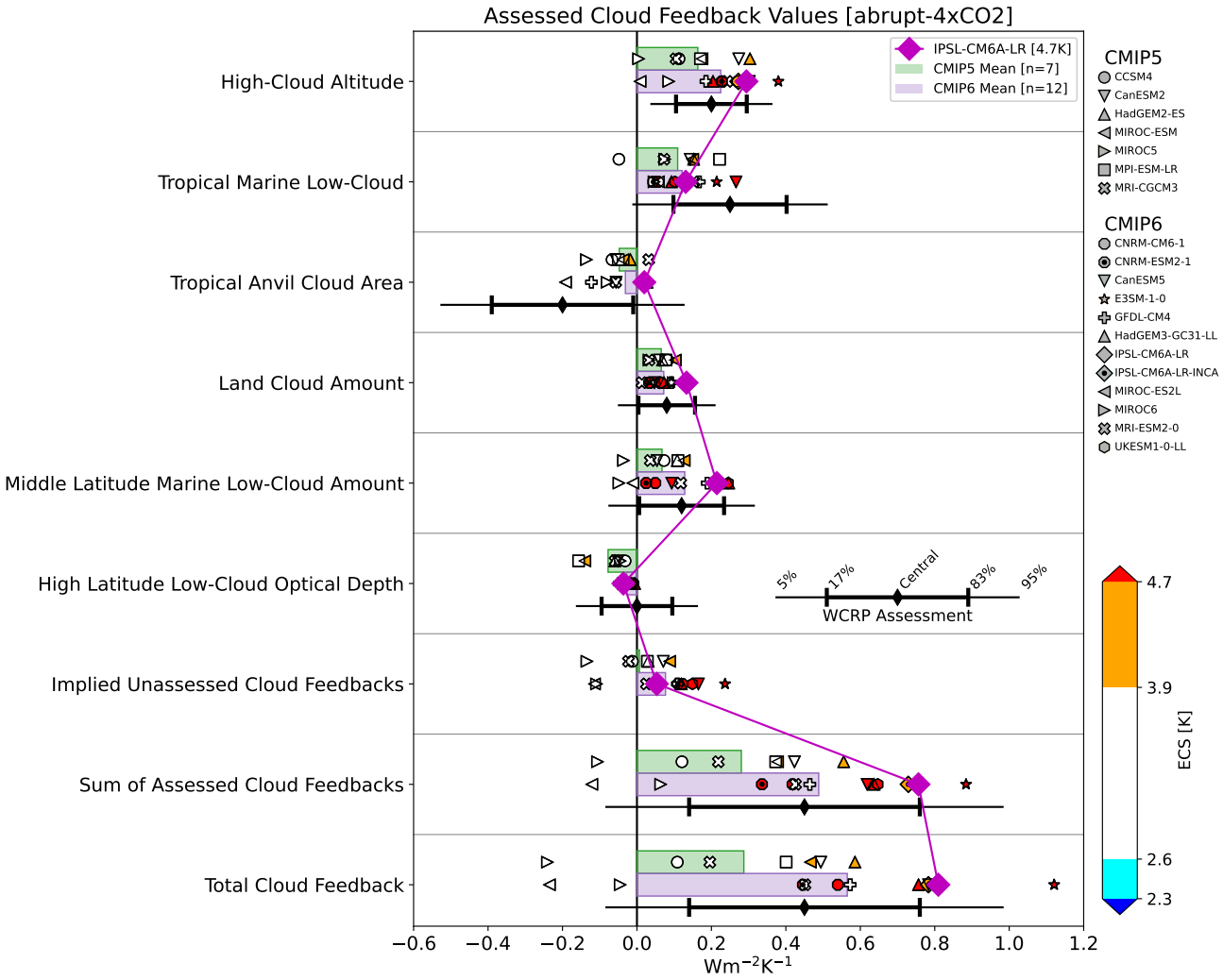

Figure S17. As in Figure 1, but highlighting IPSL-CM6A-LR.

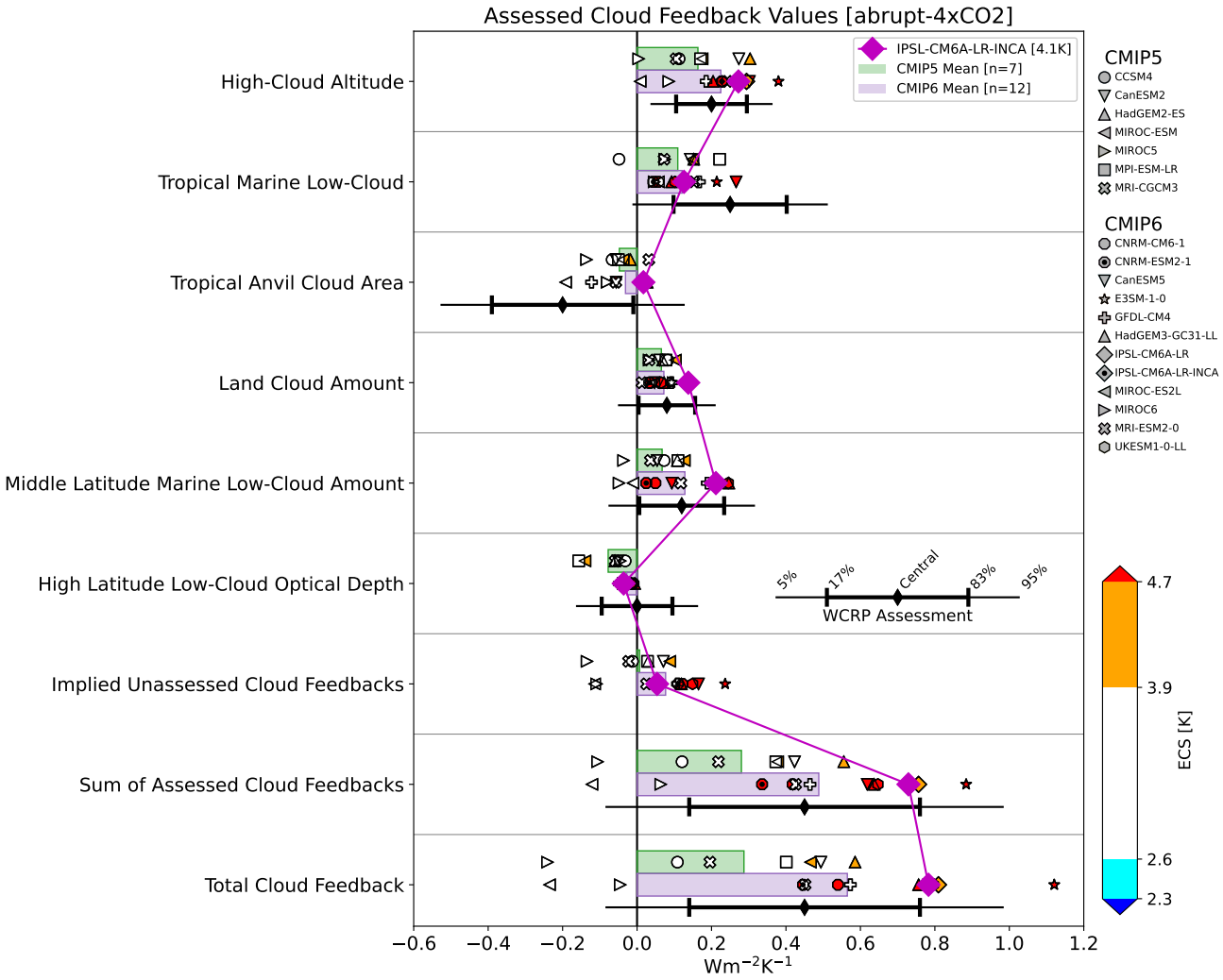

Figure S18. As in Figure 1, but highlighting IPSL-CM6A-LR-INCA.

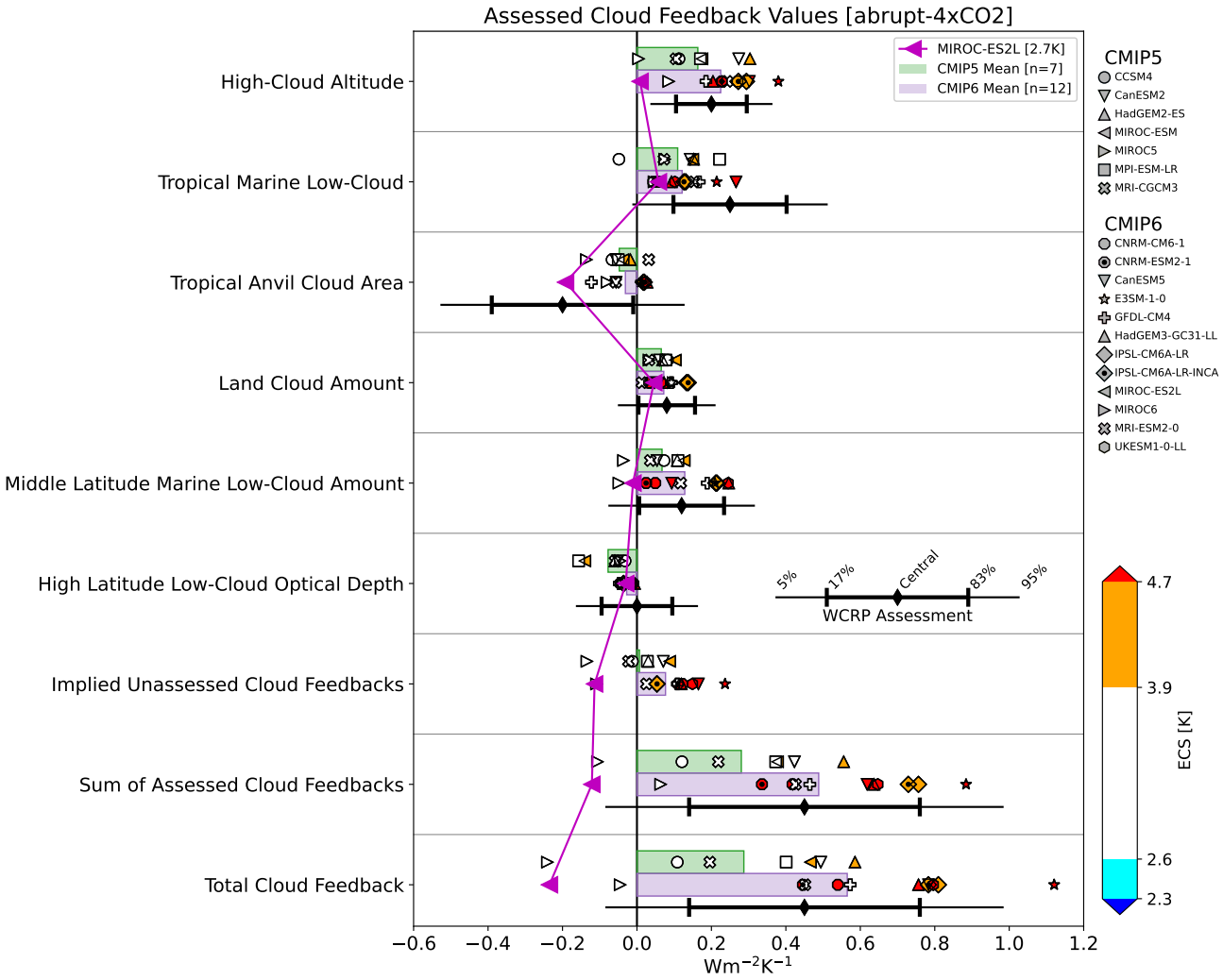

Figure S19. As in Figure 1, but highlighting MIROC-ES2L.

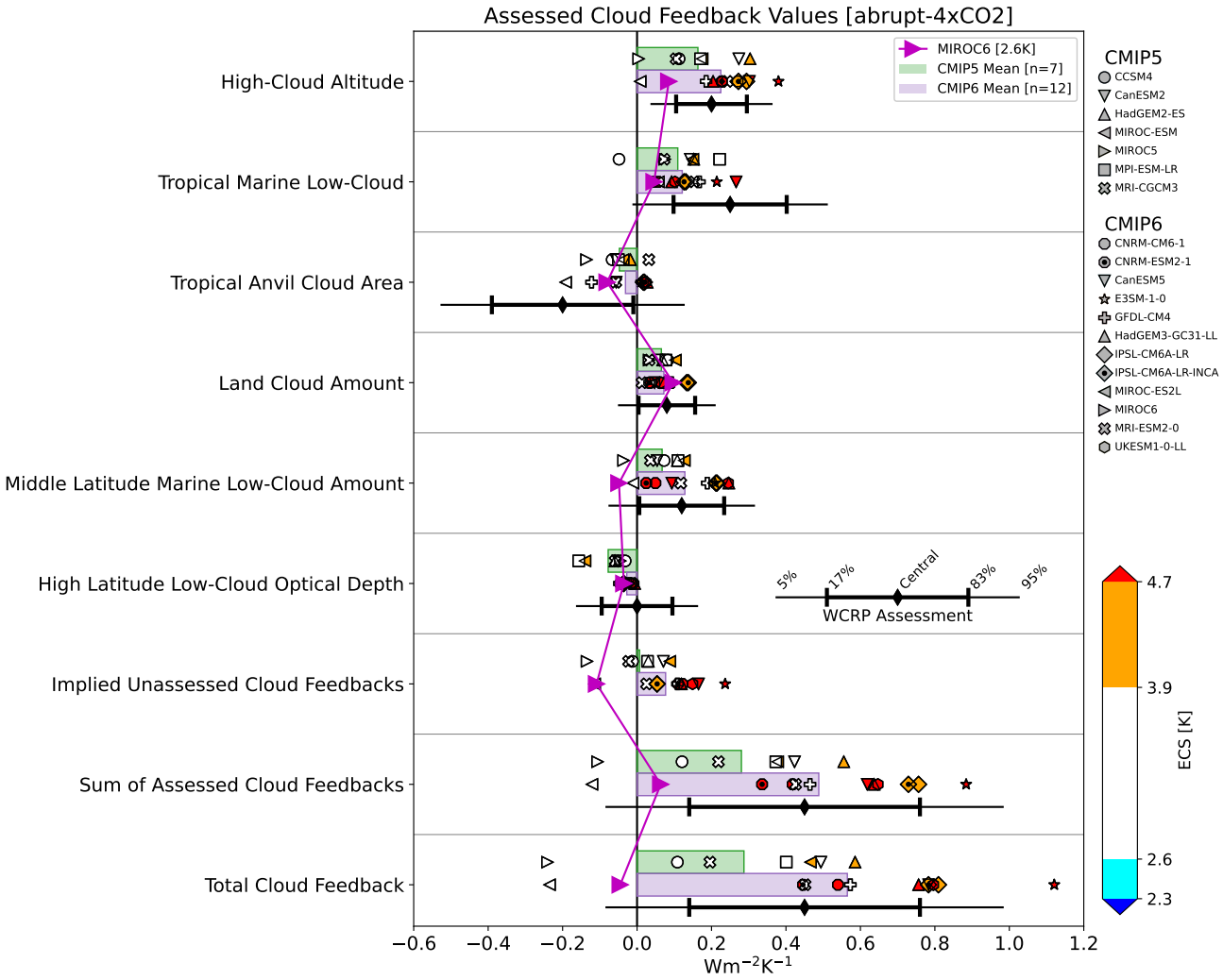

Figure S20. As in Figure 1, but highlighting MIROC6.

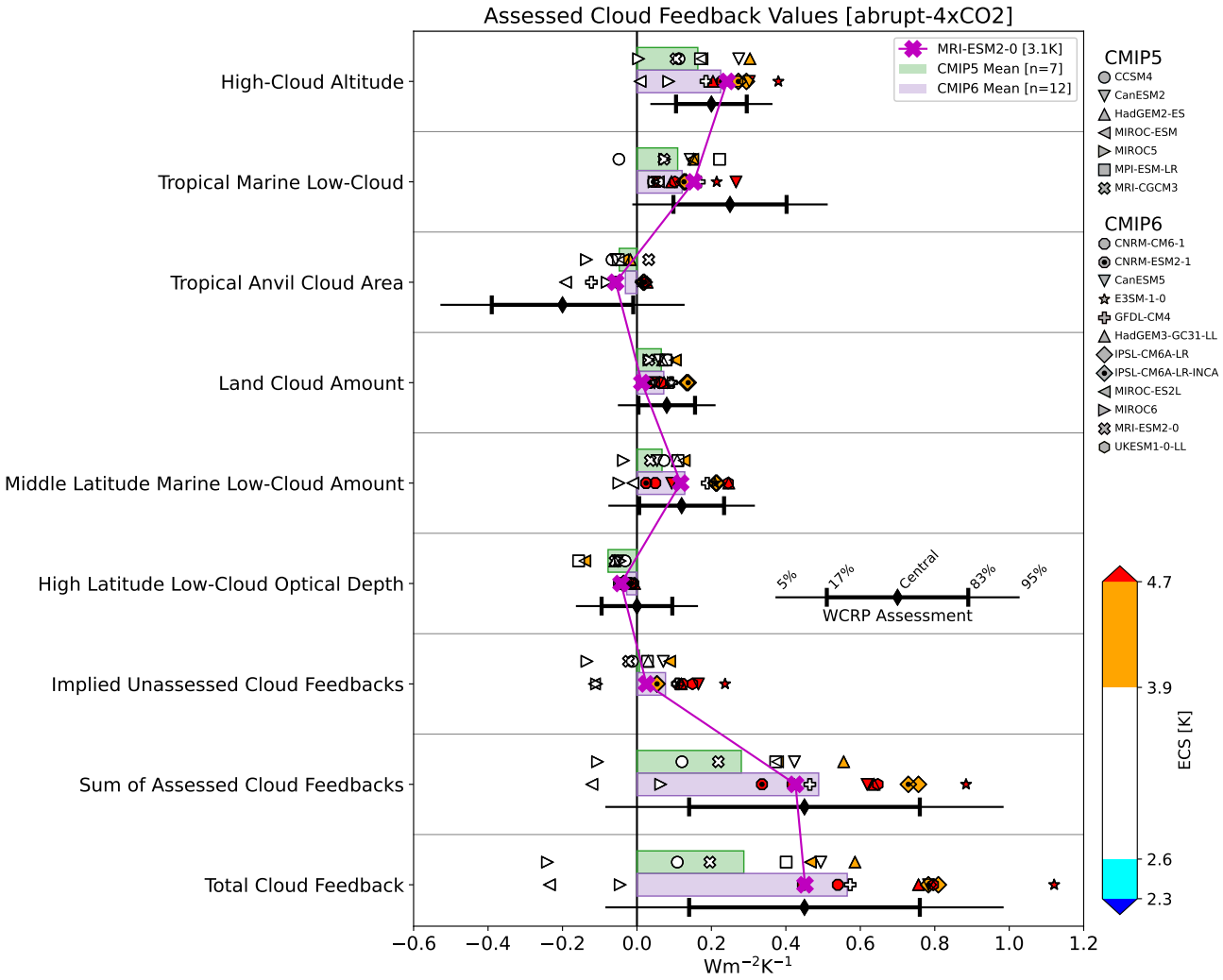

Figure S21. As in Figure 1, but highlighting MRI-ESM2-0.

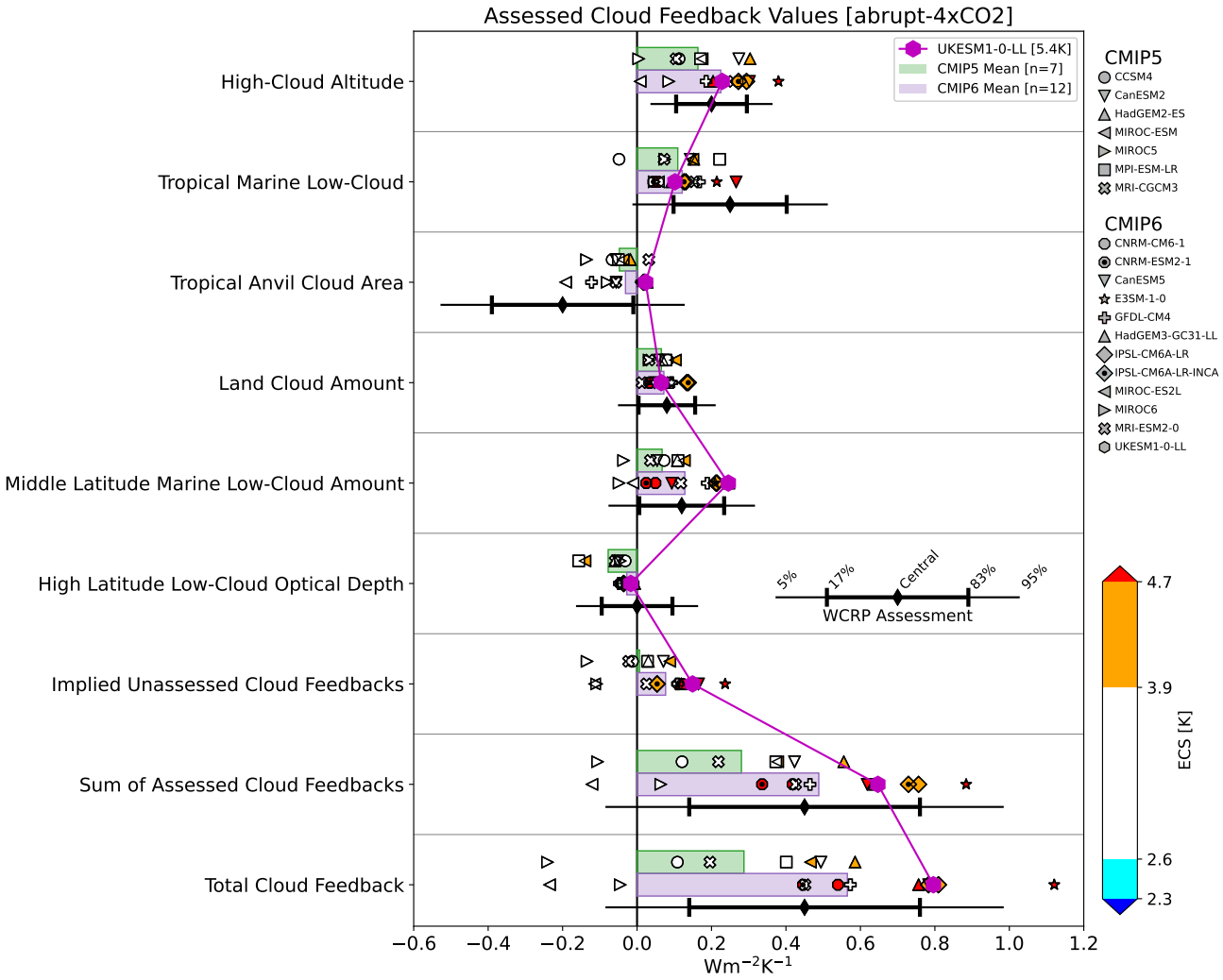

Figure S22. As in Figure 1, but highlighting UKESM1-0-LL.